POISSON KERNEL-BASED TESTS FOR UNIFORMITY ON THE D-DIMENSIONAL SPHERE

Yuxin Ding, Marianthi Markatou, Giovanni Saraceno

Department of Biostatistics, University at Buffalo,

State University of New York

Supplementary Material

S1. Tests of uniformity: a brief review

Given independent and identically distributed unit vectors $\mathbf{x}_i, i = 1, 2, .., n$, we denote our sample by $\boldsymbol{x}$= $(\mathbf{x}_1, \mathbf{x}_2, ..., \mathbf{x}_n)$, where $\mathbf{x}_i^T = (x_{i1}, x_{i2}, ..., x_{id})$, $||\mathbf{x}_i|| = 1$. Then $\bar{\mathbf{x}} = \frac{1}{n}\sum_{i=1}^{n} \mathbf{x}_i$ is called the *mean direction* of the sample. Further, the *mean resultant length* (Mardia and Jupp (2000)) is defined as

$$\bar{R} = ||\bar{\mathbf{x}}|| = \frac{1}{n}\sqrt{\left(\sum_{i=1}^{n} x_{i1}\right)^2 + \left(\sum_{i=1}^{n} x_{i2}\right)^2 + ... + \left(\sum_{i=1}^{n} x_{id}\right)^2}.$$

Rayleigh's test (Rayleigh (1919)) is proposed for testing the uniformity on circular data, i.e, data on sphere $\mathcal{S}^1$, but it is easily generalized to the higher dimensional sphere $\mathcal{S}^{d-1}$ (García-Portugués and Verdebout (2018); Figueiredo (2007)). When the d-dimensional $\mathbf{x}$ is uniformly distributed on $\mathcal{S}^{d-1}$, $E[\mathbf{x}] = \mathbf{0}$. Rayleigh's test rejects the null hypothesis of uniformity when the value of $\bar{R}$ is large. A commonly used Rayleigh's test statistic is R_n, which has an asymptotic χ^2_d distribution under the null hypothesis of uniformity, and where

$$R_n = dn\bar{R}^2 = \frac{d}{n}\left[\left(\sum_{i=1}^{n} x_{i1}\right)^2 + \left(\sum_{i=1}^{n} x_{i2}\right)^2 + ... + \left(\sum_{i=1}^{n} x_{id}\right)^2\right].$$

Further discussion of the properties of Rayleigh's test can be found in Mardia and Jupp (2000) and García-Portugués and Verdebout (2018).

Ajne (1968) proposed a test for uniformity of a circular distribution, and Prentice (1978) extended it to the $\mathcal{S}^{d-1}$ sphere. The computational form of Ajne's test statistic is:

$$\begin{aligned} A_n &= \frac{4}{n} - \frac{1}{n\pi} \sum_{1 \le i < j \le n} cos^{-1}\left(\mathbf{x}_i^T \mathbf{x}_j\right) \\ &= \frac{4}{n} - \frac{1}{n\pi} \sum_{i=1}^{n} \sum_{j=2}^{i-1} cos^{-1}\left(\sum_{k=1}^{d} x_{ik} x_{jk}\right). \end{aligned}$$

The asymptotic distribution of A_n, under the null hypothesis of uniformity, is an infinite linear combination of independent χ^2_1 variables.

Giné's test statistic (Giné (1975); Prentice (1978)) for uniformity on the sphere $\mathcal{S}^{d-1}$ has the form:

$$\begin{aligned} G_n &= \frac{2}{n} - \frac{d-1}{2n}\left[\frac{\Gamma((d-1)/2)}{\Gamma(d/2)}\right]^2 \sum_{1 \le i < j \le n} sin\left[cos^{-1}\left(\mathbf{x}_i^T \mathbf{x}_j\right)\right] \\ &= \frac{2}{n} - \frac{d-1}{2n}\left[\frac{\Gamma((d-1)/2)}{\Gamma(d/2)}\right]^2 \sum_{i=1}^{n} \sum_{j=2}^{i-1} sin\left[cos^{-1}\left(\sum_{k=1}^{d} x_{ik} x_{jk}\right)\right]. \end{aligned}$$

Asymptotically, the distribution of G_n is an infinite linear combination of independent χ^2_1 variables under the null hypothesis of uniformity.

Bingham's test is proposed based on the fact that when $\mathbf{x}$ is uniformly distributed, $E[\mathbf{x}\mathbf{x}^\mathbf{T}] = \frac{1}{d} I_d$, where I_d is an identity matrix of size d (Bingham (1974)). Then Bingham's test statistic is:

$$\begin{aligned} B_n &= \frac{1}{2}nd(d+2)\left\{tr\left[(\frac{1}{n}\sum_{i=1}^{n}\mathbf{x}_i^T\mathbf{x}_i)^2\right] - \frac{1}{d}\right\} \\ &= \frac{1}{2}nd(d+2)\left[\frac{1}{n}\sum_{k=1}^{d}\left(\sum_{i=1}^{n}x_{ik}^2\right)^2 - \frac{1}{d}\right]. \end{aligned}$$

Bingham's test statistic has an asymptotic distribution $\chi^2_{(d-1)(d+2)/2}$ under the null hypothesis of uniformity.

Various papers compare the power of the different tests of uniformity. To mention only a few works Figueiredo and Gomes (2003) compared the power of Bingham and Giné's tests of uniformity versus a Bingham or a mixture of Bingham populations for a variety of dimensions and sample sizes and concluded that the two tests have identical power for the cases studied. Figueiredo (2007) also used the von Mises distribution as an alternative to the uniform distribution, while recently Cutting et al. (2020) considered the non-null behavior of axial tests of uniformity. Finally, Jammalamadaka et al. (2020) proposed tests of uniformity that detect well multimodal mixtures of von Mises distributions.

S2. The Poisson kernel or exit on the sphere density

Golzy and Markatou (2020) used the Poisson kernel-based density (PKBD) and constructed clustering algorithms appropriate for clustering directional data and data vectors that are standardized. Golzy and Markatou (2020) presented connections of the PKBD with other distributions on the sphere and defined the PKBD as:

$$f(\mathbf{x}; \rho, \boldsymbol{\mu}) = \frac{1 - \rho^2}{w_d \|\mathbf{x} - \rho\boldsymbol{\mu}\|^d}, \tag{S2.1}$$

where $1 < \rho < 1, \mu \in \mathcal{S}^{d-1}$ a vector orienting the center of the distribution. The parameter ρ controls the concentration of the distribution around the vector $\boldsymbol{\mu}$, and it is related to the variance of the distribution. Furthermore, $w_d = 2\pi^{d/2}$. $\{\Gamma(d/2)\}^{-1}$ is the surface area of the unit sphere in $\mathbb{R}^d$, so that it is ensured that $f(\mathbf{x}; \rho, \boldsymbol{\mu})$ integrates to 1.

The PKBDs are unimodal and symmetric around $\boldsymbol{\mu}$. Figure S3 shows the shape of these densities as a function of the concentration parameter ρ in two dimensions. Note that, for smaller values of ρ the distribution is approximately uniform, while as $\rho \to 1$ there are pronounced peaks of mass.

Golzy and Markatou (2020) showed that the two-dimensional PKBD is related to the projected normal distribution with mean $\mathbf{0}$. It also equals the Kato and McCullagh family of densities for $d = 2$ (Kato and McCullagh (2018)), as both Kato and McCullagh and PKBDs for $d = 2$ reduce to the wrapped Cauchy family of densities.

For dimension $d > 2$, the PKBD is the exit distribution on the sphere, proposed by Kato and Jones (2013). This distribution is called an exit distribution because it represents the distribution of the position where a d-dimensional Brownian particle first hits the unit circle, given the future point at which the particle exits a circle with a larger radius (see Kato and Jones (2013), eq.(13), p. 169).

S3. Technical Details

S3.1 Notation

We present the notation we will use, and relevant definitions.

A twice continuously differentiable, complex-valued function f defined on an open, non-empty subset of $\mathbb{R}^d$ is harmonic if $\triangle f = 0$, where $\triangle = D_1^2 + \cdots + D_d^2$ and D_j^2 is the second partial derivative with respect to the j^{th} coordinate variable. The Poisson kernel $P_\eta(\mathbf{x}, \mathbf{y})$ as a function of $\mathbf{x}$ for fixed $\mathbf{y} \in \mathcal{S}^{d-1}$ is harmonic on $\mathbb{R}^d \setminus \{\mathbf{y}\}$ (see p.13 of Axler et al. (2001)).

Let $\mathcal{P}_m(\mathbb{R}^d)$ denote the complex vector space of all homogeneous polynomials on $\mathbb{R}^d$ of degree m, and $\mathcal{H}_m(\mathbb{R}^d)$ denotes the subspace of $\mathcal{P}_m(\mathbb{R}^d)$ consisting of all homogeneous harmonic polynomials on $\mathbb{R}^d$ of degree m. The restriction of the subspace $\mathcal{H}_m(\mathbb{R}^d)$ to the d-dimensional sphere $\mathcal{S}^{d-1}$ has its own name and notation. A spherical harmonic of degree m is the restriction to $\mathcal{S}^{d-1}$ of an element of $\mathcal{H}_m(\mathbb{R}^d)$. The collection of all spherical harmonics of degree m is denoted by $\mathcal{H}_m(\mathcal{S}^{d-1})$ and is defined as $\mathcal{H}_m(\mathcal{S}^{d-1}) = \{p|_{\mathcal{S}^{d-1}} : p \in \mathcal{H}_m(\mathbb{R}^d)\}$.

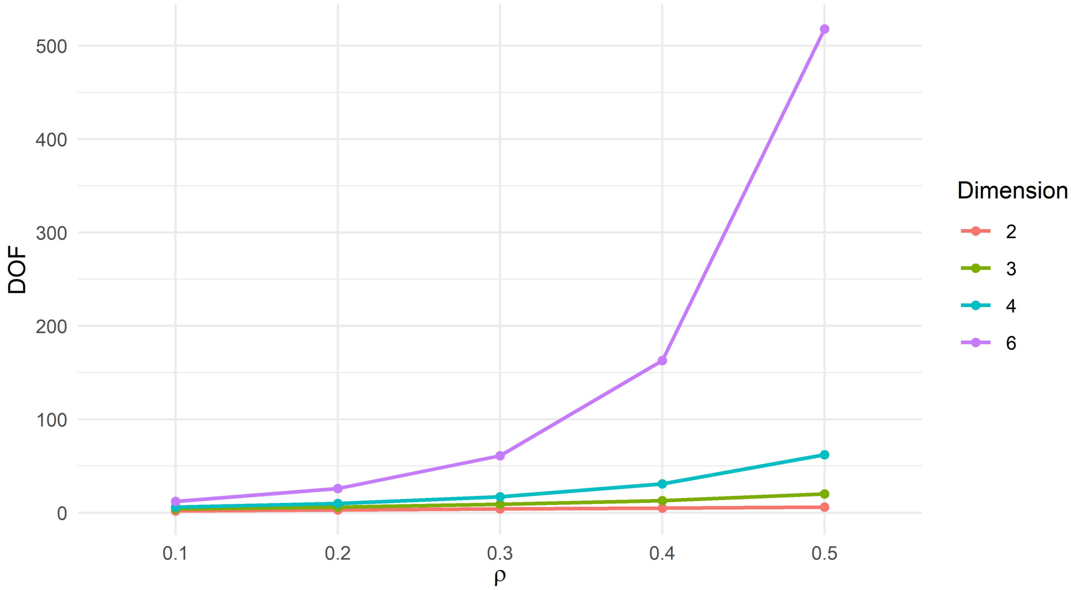

Figure S1: The DOF of the d-dimensional centered Poisson kernel versus the tuning parameter ρ, when the dimension of the data is 2, 3, 4 and 6.

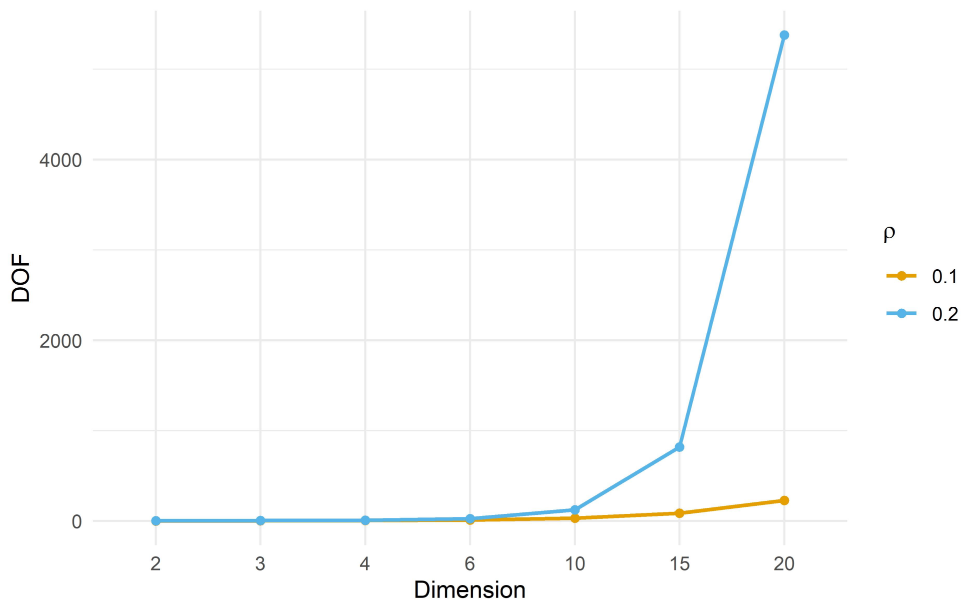

Figure S2: The DOF of the d-dimensional centered Poisson kernel versus the dimension of the data when the tuning parameter $\rho = 0.1$ and 0.2 respectively.

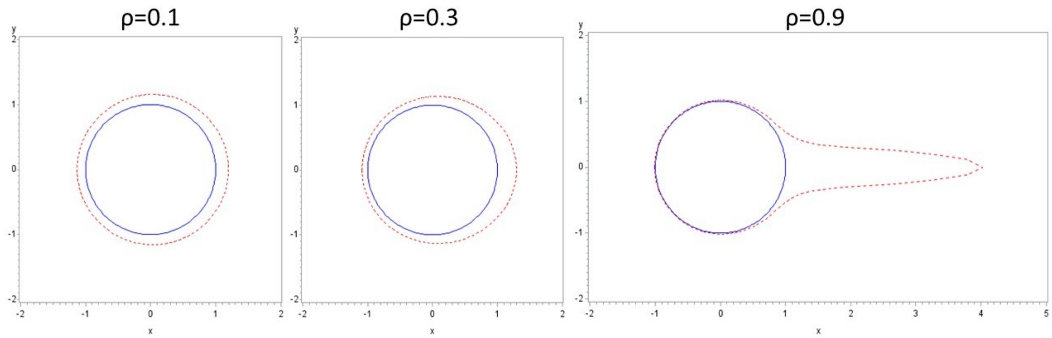

Figure S3: Scaled 2-dimensional PKBD with ρ=0.1, 0.3, 0.9.

Denote by $L^2(\mathcal{S}^{d-1})$ the usual Hilbert space of Borel-measurable, square-integrable functions on $\mathcal{S}^{d-1}$ with inner product defined by $\langle f, g\rangle = \int_{\mathcal{S}^{d-1}} f \cdot g d\sigma$, where σ is the normalized surface measure on $\mathcal{S}^{d-1}$. View now $\mathcal{H}_m(\mathcal{S}^{d-1})$ as an inner product space with the $L^2(\mathcal{S}^{d-1})$ inner product defined above. Fix a point $b \in \mathcal{S}^{d-1}$ and consider the linear map $\Lambda : \mathcal{H}_m(\mathcal{S}^{d-1}) \to \mathbb{R}$ defined by $\Lambda(p) = p(b)$. The finite dimensionality of $\mathcal{H}_m(\mathcal{S}^{d-1})$ guarantees the existence of a unique function $Z_m(\cdot, b) \in \mathcal{H}_m(\mathcal{S}^{d-1})$ such that

$$p(b) = \langle p, Z_m(\cdot, b)\rangle = \int_{\mathcal{S}^{d-1}} p(\zeta) Z_m(\zeta, b) d\sigma(\zeta), \forall p \in \mathcal{H}_m(\mathcal{S}^{d-1}).$$

The spherical harmonic $Z_m(\cdot, b)$ is called the zonal harmonic of degree m with pole b. Zonal harmonics are the eigenfunctions of the Poisson kernel decomposition and are harmonic polynomials defined on $\mathcal{S}^{d-1}$. Some basic properties of zonal harmonics are discussed on p.95 of Axler et al. (2001).

S3.2 Proofs

Proof of Lemma 1. By definition of the Poisson integral, the left hand side of the above relationship equals $P\left[P(\mathbf{z},\cdot)\right]$. Therefore, we only need to prove that, for any fixed $\mathbf{z}$, the right side of the above integral is a harmonic function of $\mathbf{x}$ and matches $P(\mathbf{z},\cdot)$ on the sphere $\mathcal{S}$. First, the right hand side of the integral equals $P(\|\mathbf{z}\|\mathbf{x}, \mathbf{z}/\|\mathbf{z}\|)$ and this is a harmonic function.

By definition, the Poisson kernel is given as

$$P_\rho(\mathbf{u},\mathbf{v}) = P(\rho\mathbf{u},\mathbf{v}) = \frac{1-\rho^2}{(1+\rho^2-2\rho\mathbf{u}\mathbf{v})^{d/2}}, \qquad \mathbf{u},\mathbf{v} \in \mathcal{S}^{d-1}.$$

Notice that in the above expression $\rho^2 = ||\rho\mathbf{u}||^2 = \rho^2||\mathbf{u}||^2 = \rho^2$, since $\mathbf{u} \in \mathcal{S}^{d-1}$ so $||\mathbf{u}||^2 = 1$.

In our case, $\rho\mathbf{u} = ||\mathbf{z}||\mathbf{x}$, so $||\ ||\mathbf{z}||\ \mathbf{x}\ ||^2 = ||\mathbf{z}||^2||\mathbf{x}||^2 = \rho^2$ and $\rho\mathbf{u}\cdot\mathbf{v} = ||\mathbf{z}||\mathbf{x}\cdot\frac{\mathbf{z}}{||\mathbf{z}||} = \mathbf{x}\cdot\mathbf{z}$. Hence we have,

$$\frac{1-||\mathbf{x}||^2||\mathbf{z}||^2}{(1+||\mathbf{x}||^2||\mathbf{z}||^2-2\mathbf{x}\cdot\mathbf{z})^{d/2}} = P(||\mathbf{z}||\mathbf{x}, \mathbf{z}/||\mathbf{z}||).$$

Also, when $\mathbf{x} \in \mathcal{S}^{d-1}$, $\|\mathbf{x}\| = 1$ and hence

$$\frac{1-\|\mathbf{x}\|^2\cdot\|\mathbf{z}\|^2}{\left(1-2\mathbf{x}\cdot\mathbf{z}+\|\mathbf{x}\|^2\cdot\|\mathbf{z}\|^2\right)^{d/2}} = \frac{1-\|\mathbf{z}\|^2}{\left(1-2\mathbf{x}\cdot\mathbf{z}+\|\mathbf{z}\|^2\right)^{d/2}} = P(\mathbf{x},\mathbf{z}).$$

This completes the proof. □

Proof of Lemma 2. Recall that the Poisson kernel is a density and so

$$\int_{\mathcal{S}} P(\mathbf{u},\boldsymbol{\zeta})d\sigma(\boldsymbol{\zeta}) = 1.$$

Moreover, for every $d \geq 2$ the Poisson kernel can be written as

$$P(\mathbf{u}, \boldsymbol{\zeta}) = \sum_{m=0}^{\infty} Z_m(\mathbf{u}, \boldsymbol{\zeta}),$$

$\forall \mathbf{u} \in \mathcal{B}^d$, $\boldsymbol{\zeta} \in \mathcal{S}$ (see theorem 5.33 on p. 99 of Axler et al. (2001)). Therefore, we can write:

$$\int_{\mathcal{S}} \sum_{m=0}^{\infty} Z_m(\mathbf{u}, \boldsymbol{\zeta}) d\sigma(\boldsymbol{\zeta}) = \int_{\mathcal{S}} Z_0(\mathbf{u}, \boldsymbol{\zeta}) d\sigma(\boldsymbol{\zeta}) + \sum_{m=1}^{\infty} \int_{\mathcal{S}} Z_m(\mathbf{u}, \boldsymbol{\zeta}) d\sigma(\boldsymbol{\zeta}).$$

Because $Z_0(\mathbf{u}, \boldsymbol{\zeta}) = 1$, the above relationship is equivalent to writing

$$1 = 1 + \sum_{m=1}^{\infty} \int_{\mathcal{S}} Z_m(\mathbf{u}, \boldsymbol{\zeta}) d\sigma(\boldsymbol{\zeta}),$$

from which we obtain

$$\sum_{m=1}^{\infty} \int_{\mathcal{S}} Z_m(\mathbf{u}, \boldsymbol{\zeta}) d\sigma(\boldsymbol{\zeta}) = 0.$$

Therefore, $\forall m \geq 1$ we obtain

$$\int_{\mathcal{S}} Z_m(\mathbf{u}, \boldsymbol{\zeta}) d\sigma(\boldsymbol{\zeta}) = 0.$$

□

Proof of Lemma 3. Consider a real orthonormal nasis $e_1, e_2, \cdots, e_{d_{d,m}}$ of the space $\mathcal{H}_m(\mathcal{S})$ where $d_{d,m} = dim\mathcal{H}_m(\mathcal{S}) = dim\mathcal{H}_m(\mathbb{R}^d)$. This basis exists and can be constructed by applying the techniques described on p. 92 of Axler et al. (2001). Then we can write:

$$Z_m(\mathbf{u}, \boldsymbol{\zeta}) = \sum_{j=1}^{d_{d,m}} e_j(\mathbf{u}) e_j(\boldsymbol{\zeta}),$$

and

$$Z_m^2(\mathbf{u},\boldsymbol{\zeta}) = \sum_{j=1}^{d_{d,m}} e_j^2(\mathbf{u})e_j^2(\boldsymbol{\zeta}).$$

Therefore, we obtain:

$$\sum_{j=1}^{d_{d,m}} \int_{\mathcal{S}} e_j^2(\mathbf{u})e_j^2(\boldsymbol{\zeta})d\sigma(\mathbf{u})d\sigma(\boldsymbol{\zeta}) = \sum_{j=1}^{d_{d,m}} \left(\int_{\mathcal{S}} e_j^2(\mathbf{u})d\sigma(\mathbf{u})\right)\left(\int_{\mathcal{S}} e_j^2(\boldsymbol{\zeta})d\sigma(\boldsymbol{\zeta})\right) = d_{d,m}.$$

□

Proof of Lemma 4. Write

$$Z_p(\mathbf{u},\boldsymbol{\zeta}) = \sum_{j=1}^{d_{d,p}} e_j(\mathbf{u})e_j(\boldsymbol{\zeta}),$$

where $e_1, e_2, \cdots, e_{d_{d,p}}$ is a real orthogonal basis of the space $\mathcal{H}_p(\mathcal{S})$, $\mathcal{S} \in \mathbb{R}^d$. Now, assume that $p \neq q$ and that $e_1^*, e_2^*, \cdots, e_{d_{d,p}}^*$ is a real, orthonormal basis for the space $\mathcal{H}_q(\mathcal{S})$. Then

$$Z_q(\mathbf{u},\boldsymbol{\zeta}) = \sum_{j=1}^{d_{d,p}} e_j^*(\mathbf{u})e_j^*(\boldsymbol{\zeta}),$$

with $d_{d,p} = dim\mathcal{H}_p(\mathcal{S})$, $d_{d,q} = dim\mathcal{H}_q(\mathcal{S})$. Therefore

$$Z_p(\mathbf{u},\boldsymbol{\zeta})Z_q(\mathbf{u},\boldsymbol{\zeta}) = \sum_{k=1}^{d_{d,p}}\sum_{l=1}^{d_{d,q}} e_k(\mathbf{u})e_k(\boldsymbol{\zeta})e_l^*(\mathbf{u})e_l^*(\boldsymbol{\zeta}).$$

Moreover

$$\int_{\mathcal{S}} Z_p(\mathbf{u},\boldsymbol{\zeta})Z_q(\mathbf{u},\boldsymbol{\zeta})d\sigma(\mathbf{u})d\sigma(\boldsymbol{\zeta}) = \sum_{k=1}^{d_{d,p}}\sum_{l=1}^{d_{d,q}} \int_{\mathcal{S}} e_k(\mathbf{u})e_k(\boldsymbol{\zeta})e_l^*(\mathbf{u})e_l^*(\boldsymbol{\zeta})d\sigma(\mathbf{u})d\sigma(\boldsymbol{\zeta}).$$

But $e_k \in \mathcal{H}_p(\mathcal{S})$, $e_k^* \in \mathcal{H}_q(\mathcal{S})$, $p \neq q$; without loss of generality assume that $p < q$; then

$$\int_{\mathcal{S}} e_k(\mathbf{u})e_l^*(\mathbf{u})d\sigma(\mathbf{u}) = 0$$

and

$$\int_{\mathcal{S}} e_k(\boldsymbol{\zeta}) e_l^*(\boldsymbol{\zeta}) d\sigma(\boldsymbol{\zeta}) = 0$$

because e_l^* is harmonic and homogeneous and $q > p$, thus by proposition 5.9 on p.79 of Axler et al. (2001) we obtain the result that is given in the statement of the Lemma.

□

Proof of Proposition 3. Recall that

$$DOF(K_{cen}) = \frac{[tr(K_{cen})]^2}{tr(K_{cen}^2)},$$

and $tr(K_{cen}) = \int K(\mathbf{u}, \mathbf{u}) dG(\mathbf{u})$, with G being the measure with respect to which we center the kernel.

The numerator of $DOF(K_{cen})$ equals

$$\left(\frac{1+\rho}{(1-\rho)^{d-1}} - 1 \right)^2 = \frac{\left(1+\rho-(1-\rho)^{d-1}\right)^2}{(1-\rho)^{2(d-1)}}.$$

The denominator of $DOF(K_{cen})$ is

$$\frac{1+\rho^2}{(1-\rho^2)^{d-1}} - 1 = \frac{1+\rho^2-(1-\rho^2)^{d-1}}{(1-\rho^2)^{d-1}}.$$

Finally,

$$\begin{aligned} DOF(K_{cen}) &= \frac{\frac{(1+\rho-(1-\rho)^{d-1})^2}{(1-\rho)^{2(d-1)}}}{\frac{1+\rho^2-(1-\rho^2)^{d-1}}{(1-\rho^2)^{d-1}}} \\ &= \left(\frac{1+\rho}{1-\rho}\right)^{d-1} \left\{ \frac{(1+\rho-(1-\rho)^{d-1})^2}{1+\rho^2-(1-\rho^2)^{d-1}} \right\}. \end{aligned}$$

Hence, the degrees of freedom are a function of the concentration parameter $\rho, 0 < \rho < 1$, and the data dimension d. Note that when $\rho \to 0, DOF(K_{cen}) \to d$, and this can be easily obtained by applying twice L'Hôpital's rule. On the other hand, when $\rho \to 1, DOF(K_{cen}) \to \infty$. $\square$

S4. Empirical results

S4.1 Level computations

Algorithm S1: Level Calculation

1 Generate data from a Uniform distribution on the d-dimensional sphere;

2 Compute the different test statistics for 5000 Monte Carlo(MC) replications, and for sample sizes N;

3 Count the number of times t the null hypothesis of $H_0 : F \sim$ Uniform on the sphere is rejected;

4 Divide $t/$(the number of MC replications) to obtain the level of the test.

Algorithm 1 describes in details how the level is computed in the simulation study. Table S1 presents the empirical level of various tests of uniformity on the sphere, as a function of the dimension, sample size, and in the case of proposed tests tuning parameter ρ.

Table S1: Empirical level of various tests of uniformity on the sphere, presented as a function of the dimension and sample size. The table presents the levels of S_n, T_n for various tuning parameters.

Dimension	Sample size	Rayleigh	Ajne	Giné	Bingham	S_n $\rho = 0.05$	S_n $\rho = 0.1$	S_n $\rho = 0.15$	S_n $\rho = 0.2$	T_n $\rho = 0.05$	T_n $\rho = 0.1$	T_n $\rho = 0.15$	T_n $\rho = 0.2$
2	100	0.053	0.052	0.047	0.050	0.053	0.053	0.054	0.054	0.057	0.057	0.055	0.055
2	500	0.048	0.048	0.052	0.052	0.048	0.050	0.050	0.049	0.050	0.052	0.050	0.049
2	1000	0.040	0.044	0.049	0.044	0.041	0.042	0.042	0.042	0.043	0.043	0.043	0.043
3	100	0.047	0.045	0.050	0.051	0.045	0.045	0.046	0.046	0.046	0.045	0.045	0.044
3	500	0.048	0.051	0.049	0.051	0.046	0.046	0.049	0.048	0.046	0.046	0.046	0.044
3	1000	0.054	0.060	0.044	0.049	0.053	0.050	0.051	0.053	0.053	0.049	0.048	0.051
4	100	0.049	0.052	0.044	0.049	0.050	0.052	0.052	0.054	0.049	0.050	0.049	0.048
4	500	0.045	0.047	0.061	0.059	0.047	0.045	0.047	0.049	0.045	0.041	0.039	0.038
4	1000	0.053	0.056	0.051	0.050	0.053	0.050	0.054	0.054	0.051	0.048	0.049	0.045
6	100	0.048	0.050	0.052	0.053	0.052	0.055	0.057	0.058	0.050	0.050	0.050	0.051
6	500	0.055	0.055	0.052	0.053	0.055	0.057	0.058	0.058	0.055	0.055	0.052	0.050
6	1000	0.052	0.051	0.049	0.048	0.054	0.056	0.058	0.059	0.052	0.052	0.051	0.050

S4.2 The data distribution is one Poisson Kernel-Based Density:

We generate data from PKBD distribution on the d-dimensional sphere where d=2, 3, 6, 10 and with sample sizes 50, 100, 500, 1000 respectively. The concentration parameter of the underlying distribution ρ_0 is set to be 0.2 and 0.4 respectively. Table S2 presents the evaluation results in terms of power for all tests. When the sample size is 50, 100 and 500 the number of Monte Carlo replications is 1000, while for a sample size of 1000 equals 200. The reduction in the number of Monte Carlo replications is due to the fact that the PKBD sampler is slow for larger sample sizes. The proposed tests perform slightly better than Ajne and Raleigh in terms of power and outperform the Bingham and Giné tests in all cases studied. When the sample size becomes larger, all methods obtain power 1 or very high power approaching 1.

S4.3 The data distribution is a multi-component mixture of Poisson kernel-based densities:

We also study the performance of the tests in the presence of 3, 4 and 5 modes, in dimension 10. The mean vectors are orthogonal to each other. All ρ values are set to be 0.2 for simplicity. The sample size is set as 100 and 200, respectively. Table S3 shows the power of all tests. When the number of modes increases, while the sample size stays at 100 observations, the power of all tests decrease. But when the sample size increases to 200, the Rayleigh, Ajne, S_n and T_n tests can obtain about or above

S4.3 The data distribution is a multi-component mixture of Poisson kernel-based densities:

Table S2: Evaluation of all tests in terms of power when the alternative distribution is PKBD with $\rho = 0.2$ and 0.4 respectively. Dimension is 2, 3, 6 or 10. S_n, T_n are computed using the tuning parameter that produces the maximum power.

Dimension	Number of the modes	ρ_0	Sample size	Bingham	Rayleigh	Ajne	Giné	S_n	T_n
2	1	0.2	100	0.078	0.743	0.736	0.071	**0.751**	**0.755**
2	1	0.4	100	0.529	1	1	0.503	**1**	**1**
2	1	0.2	500	0.182	1	1	0.181	**1**	**1**
2	1	0.4	500	0.998	1	1	0.998	**1**	**1**
3	1	0.2	100	0.085	0.830	0.830	0.082	**0.838**	**0.836**
3	1	0.4	100	0.749	1	1	0.737	**1**	**1**
3	1	0.2	500	0.311	1	1	0.317	**1**	**1**
3	1	0.4	500	1	1	1	1	**1**	**1**
6	1	0.2	50	0.739	0.740	0.088	0.083	**0.747**	**0.737**
6	1	0.4	50	1	1	0.824	0.821	**1**	**1**
6	1	0.2	1000	1	1	0.945	0.945	**1**	**1**
6	1	0.4	1000	1	1	1	1	**1**	**1**
10	1	0.2	50	0.887	0.899	0.121	0.117	**0.890**	**0.879**
10	1	0.4	50	1	1	0.978	0.977	**1**	**1**
10	1	0.2	1000	1	1	0.995	1	**1**	**1**
10	1	0.4	1000	1	1	1	1	**1**	**1**

S4.3 The data distribution is a multi-component mixture of Poisson kernel-based densities:

Table S3: Performance of tests of uniformity against a mixture of three, four or five PKBDs in terms of power. The modes of each PKBD are orthogonal to each other. The dimension of the data is 10. S_n, T_n are computed using the tuning parameter that produces the maximum power.

Dimension	Number of the modes	ρ	Sample size	Bingham	Rayleigh	Ajne	Giné	S_n	T_n
10	3	0.2	100	0.076	0.688	0.692	0.086	**0.704**	**0.698**
10	4	0.2	100	0.052	0.552	0.556	0.056	**0.554**	**0.552**
10	5	0.2	100	0.050	0.428	0.440	0.048	**0.442**	**0.432**
10	3	0.2	200	0.130	0.970	0.976	0.132	**0.978**	**0.974**
10	4	0.2	200	0.074	0.886	0.890	0.070	**0.910**	**0.904**
10	5	0.2	200	0.048	0.792	0.802	0.044	**0.804**	**0.796**

0.8 power in all cases.

References

Ajne, B. (1968). A simple test for uniformity of a circular distribution. *Biometrika 55*(2), 343–354.

Axler, S., P. Bourdon, and R. Wade (2001). *Harmonic Function Theory*, Volume 137. New York: Springer-Verlag.

Bingham, C. (1974). An antipodally symmetric distribution on the sphere. *The Annals of Statistics*, 1201–1225.

Cutting, C., D. Paindaveine, and T. Verdebout (2020). On the power of axial tests of uniformity on spheres. *Electronic Journal of Statistics 14*(1), 2123–2154.

Figueiredo, A. (2007). Comparison of tests of uniformity defined on the hypersphere. *Statistics & Probability Letters 77*(3), 329–334.

Figueiredo, A. and P. Gomes (2003). Power of tests of uniformity defined on the hypersphere. *Communications in Statistics-Simulation and Computation 32*(1), 87–94.

García-Portugués, E. and T. Verdebout (2018). An overview of uniformity tests on the hypersphere. *arXiv preprint arXiv:1804.00286*.

Giné, E. (1975). Invariant tests for uniformity on compact riemannian manifolds based on sobolev norms. *The Annals of Statistics 3*(6), 1243–1266.

Golzy, M. and M. Markatou (2020). Poisson kernel-based clustering on the sphere: Convergence properties, identifiability, and a method of sampling. *Journal of Computational and Graphical Statistics 29*(4), 758–770.

Jammalamadaka, S. R., S. Meintanis, and T. Verdebout (2020). On sobolev tests of uniformity on the circle with an extension to the sphere. *Bernoulli 26*(3), 2226–2252.

Kato, S. and M. Jones (2013). An extended family of circular distributions related to wrapped cauchy distributions via brownian motion. *Bernoulli 19*(1), 154–171.

Kato, S. and P. McCullagh (2018). Möbius transformation and a cauchy family on the sphere. *arXiv preprint arXiv:1510.07679*.

Mardia, K. V. and P. E. Jupp (2000). *Directional Statistics*, Volume 2. Wiley Online Library.

Prentice, M. (1978). On invariant tests of uniformity for directions and orientations. *The Annals of Statistics*, 169–176.

Rayleigh, L. (1919). Xxxi. on the problem of random vibrations, and of random flights in one, two, or three dimensions. *The London, Edinburgh, and Dublin Philosophical Magazine and Journal of Science 37*(220), 321–347.